

PAPER

An Accurate Imaging Algorithm with Scattered Waveform Estimation for UWB Pulse Radars

Shouhei KIDERA^{†a)}, *Student Member*, Takuya SAKAMOTO^{††}, *Member*, Satoshi SUGINO^{†††}, *Nonmember*, and Toru SATO[†], *Member*

SUMMARY UWB pulse radars that offer target shape estimation are promising as imaging techniques for household or rescue robots. We have already proposed an efficient algorithm for a shape estimation method SEABED which is a fast algorithm based on a reversible transform. SEABED extracts quasi wavefronts from received signals with the filter that matches the transmitted waveform. However, the scattered waveform is, in general, different from the transmitted one depending on the shape of targets. This difference causes estimation errors in SEABED. In this paper, we propose an accurate algorithm for a polygonal-target based on scattered waveform estimation. The proposed method is presented first, followed by results of numerical simulations and experiments that show the efficiency of the proposed method.

key words: UWB pulse radar systems, SEABED, scattered waveform estimation, accurate shape estimation

1. Introduction

Development of robotics is aiming at advanced robots that can measure their surrounding environment accurately. A radar imaging has a high range resolution, and it can estimate object shapes even in the case of a fire where optical methods cannot be used. UWB (Ultra Wide-band) signals were standardized by FCC (Federal Communication Committee) in 2002 which lead to high range resolution radar systems. UWB signals have great potential for a high-resolution imaging which cannot be achieved with narrow band signals.

While many imaging algorithms for radar systems have been proposed [1]–[4], they have excessive calculation costs. To solve this problem, we proposed SEABED (Shape Estimation Algorithm based on BST and Extraction of Directly scattered waves), [5], [6], which is based on a reversible transform BST (Boundary Scattering Transform) between the time delay of received echoes and the target shape. SEABED offers fast target imaging. However, the accuracy of this method is limited because it assumes that the scattered waveform is the same as the transmitted one.

Manuscript received August 25, 2005.

Manuscript revised February 10, 2006.

[†]The authors are with the Department of Communications and Computer Engineering, Graduate School of Informatics, Kyoto University, Kyoto-shi, 606-8501 Japan.

^{††}The author is with the Department of Intelligence Science and Technology, Graduate School of Informatics, Kyoto University, Kyoto-shi, 606-8501 Japan.

^{†††}The author is with the New Product Technologies Development Department, Matsushita Electric Works, Ltd., Osaka, Japan.

a) E-mail: kidera@aso.cce.i.kyoto-u.ac.jp

DOI: 10.1093/ietcom/e89-b.9.2588

The resolution of SEABED deteriorates especially around the target edges because of the waveform differences.

To solve this problem we propose an estimation method of scattered waveforms from polygonal targets in this paper. Additionally, by utilizing the scattered waveform estimation, we propose an accurate target estimation algorithm for polygonal targets. We explain the proposed method and simulation results. We evaluate the proposed method by numerical simulations and experiments. These evaluations clarify that the proposed method achieves a remarkable accuracy of the estimation of the target shape and location. Additionally, the performance of the proposed method is not limited by the material of the target. Moreover the accuracy of this method hardly depends on the amplitude of the reflection wave.

2. System Model

We show the system model in Fig. 1. We deal with 2-dimensional problems and TE mode waves. We assume a non-dispersive and a lossless medium. We assume that the propagation speed of the radio wave is known, and that a target has a uniform complex permittivity which should be different from that of an air and is surrounded by finite linear boundaries. We utilize a mono-static radar system. An omni-directional antenna is scanned along a straight line. The current waveform at the transmitting antenna is a mono-cycle pulse. We define the parameter (x, y) as the real space where targets and antennas are located. We normalize the parameter (x, y) by λ which is the center wavelength of the transmitted current and the time scale by its period $T = \lambda/c$,

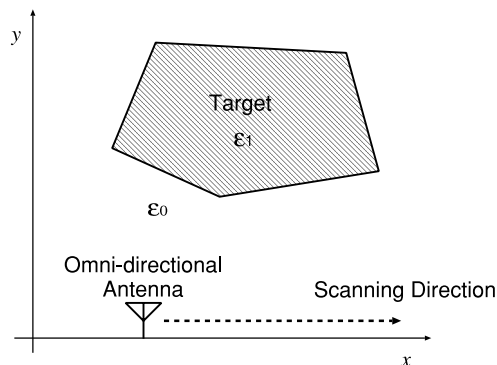


Fig. 1 System model.

where c is the speed of light.

3. Proposed Target Shape Estimation Method

In this section, we explain a shape estimation algorithm for polygonal targets. In this method, we iterate a shape estimation and a scattered waveform estimation alternately. First, we explain the necessity of a scattered waveform estimation for an accurate shape estimation. Next, we explain the procedure of the initial shape estimation and an iterative shape estimation method based on a scattered waveform estimation.

3.1 Characteristics of Scattered Waveforms from Polygonal Pillars

In general, the scattered waveform from a large planar boundary whose length is much longer than the wavelength has the same waveform as the transmitted one with the opposite sign. The scattered waveform from a ridge point of a target is different from a waveform of the transmitted one. We show the differences of these two waveforms in Fig. 2. The general scattered waveform from a polygonal pillar is a complex one influenced by these effects. SEABED algorithm has an estimation error caused by this waveform difference because it utilizes the filter matched to the transmitted waveform. In order to enhance the estimation accuracy of the target shape we must estimate the scattered waveforms.

3.2 Iterative Target Shape Estimation with Scattered Waveform Estimation

In this section, we propose an shape estimation method based on a scattered waveform estimation. Figure 3 shows the flowchart of this method. We explain the detail of the proposed method as follows. We assume that a mono-static antenna is scanned along the x axis, and the target is set at $y \geq 0$ for simplicity. We define the antenna location as $(X, 0)$ and the transmitted waveform in the frequency domain as $E_0(\omega)$, where ω is the angular frequency. We measure the time of arrival $\tau(X)$ at $(X, 0)$ as

$$\tau(X) = \arg \max_{\tau_0} \left| \int_{-\infty}^{\infty} R(\omega, X) E_0(\omega)^* e^{j\omega\tau_0} d\omega \right|, \quad (1)$$

where $R(\omega, X)$ is the received waveform at $(X, 0)$ in the frequency domain, and we define that $\arg \max$ is the value of the given argument for which the value of the given expression attains the maximum value. The integral of Eq. (1) means convolution of the reference waveform and the received signal. In this paper, we propose the shape estimation method to enhance the accuracy of the one of the edges of the polygon. This method can be easily expanded to the polygonal shape estimation by increasing the shape parameters. We define the shape parameters Z_t as

$$Z_t = (x_p, y_p, \phi_1, \phi_2, W_1, W_2), \quad (2)$$

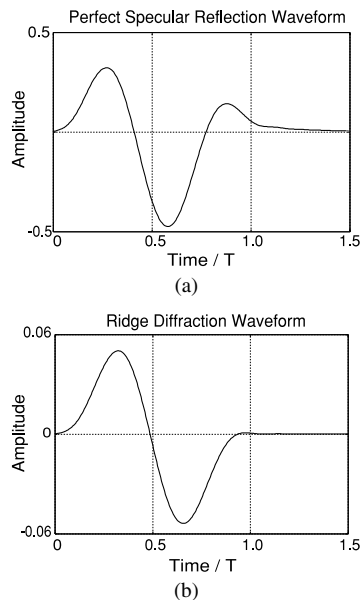


Fig. 2 Differences of the scattered waveforms.

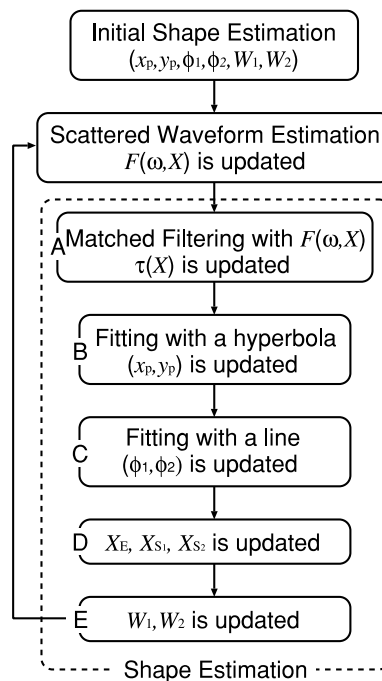


Fig. 3 Flowchart of the proposed method.

where (x_p, y_p) is the edge position, $\phi_i, (i = 1, 2)$ is each angle of the target boundary to the scanning line, which is defined as the range of $-\pi/2 < \phi_i \leq \pi/2$, and W_i is each width of the target boundary as shown in Fig. 4.

Let us explain one of the initial shape estimation methods for the proposed method. Any method which can specify Z_t can be applied to the proposed method as an initial shape estimation. We assume that the width of each plain which constitutes the target is much longer than the wavelength and the target has at least one edge, between two flat

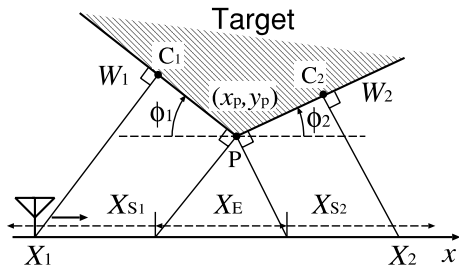


Fig. 4 Arrangement of the target location and antenna in the proposed method.

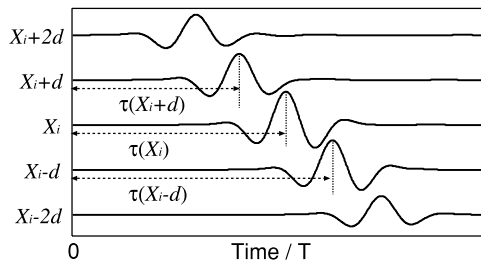


Fig. 5 Responses of the matched filter at each antenna location.

boundaries. Under this assumption, we observe a peak in the scattered echo power from the center of the plain boundary. We thus obtain two local maxima of the matched filter. We define the location of the antennas as $(X_i, 0)$, $(i = 1, 2)$, which receive the echoes from the center points C_i of the plain boundaries as shown in Fig. 4. We calculate ϕ_i from measured $\tau(X_i - d)$ and $\tau(X_i + d)$, where d is the sampling interval of scanning. Figure 5 shows examples of the responses of the matched filter at one of the two points. We calculate (x_p, y_p) as the intersection of the two boundaries. We also calculate W_i as $W_i = 2\overline{PC_i}$, where $P = (x_p, y_p)$.

Next, we explain the proposed method based on a scattered waveform estimation. With Z_t obtained by the initial shape estimation, we determine the scanning range X_{S_1} , X_{S_2} and X_E as shown in Fig. 4. We call the scattered waveform received at X_{S_1} and X_{S_2} as the specular reflection waveform, and call one at X_E as the edge diffraction waveform. In each region, we estimate the scattered waveforms from the estimated Z_t . These waveform estimation methods are explained in the next section. We define the estimated waveform at each antenna location as $F(\omega, X)$ in the frequency domain. We show the procedures of the shape estimation method as follows.

- Step A). Update the time of arrival $\tau(X)$ with the matched filter of $F(\omega, X)$ instead of $E_0(\omega)$ in Eq. (1).
- Step B). Update (x_p, y_p) by fitting with a hyperbola for estimated $\tau(X)$ as

$$(x_p, y_p) = \arg \min_{(x,y)} \sum_{X \in X_E} P(X) \left| \tau(X) - \tau_\alpha(X, x, y) \right|^2, \quad (3)$$

$$\tau_\alpha(X, x, y) = 2 \sqrt{(x - X)^2 + y^2}, \quad (4)$$

where $P(X)$ is the maximum value of the response of the matched filter at $(X, 0)$.

- Step C). Update the target angles ϕ_1, ϕ_2 of the boundaries with a common end (x_p, y_p) by fitting with a straight line for estimated $\tau(X)$ as,

$$\phi_i = \arg \min_{\phi} \sum_{X \in X_{S_i}} P(X) \left| \tau(X) - \tau_\beta(X, \phi_i) \right|^2, \quad (5)$$

$$\tau_\beta(X, \phi_i) = \frac{2 |\tan \phi_i (X - x_p) + y_p|}{\sqrt{1 + \tan^2 \phi_i}}, \quad (6)$$

where $i = 1, 2$.

- Step D). Update the scanning range X_E, X_{S_i} from the updated (x_p, y_p, ϕ_i) .
- Step E). Update X_i from the responses of the matched filter and calculate W_i .

We iterate the shape and the waveform estimation for M times to accomplish an accurate shape estimation.

4. Waveform Estimation Methods for Target Shape Estimation

4.1 Waveform Estimation with the Green's Function Integral

In this section, we explain the waveform estimation in the proposed method. In general, the specular reflection waveform from the planar boundary whose width is on the order of the wavelength is different from the transmitted one. This is because the Fresnel zone size in a high frequency band is smaller than one in a low frequency band. Many methods for the waveform estimation have been proposed, such as FDTD method and Physical Optics method. FDTD method achieves the high accuracy of the waveform estimation, but requires an intensive computation. On the other hand, Physical Optics method achieves a fast waveform estimation. However we confirm that this method has an estimation error for the edge diffraction waveform estimation for the current situation. This is because this method assumes that the size of the target is much larger than the wavelength. To accomplish a fast and an accurate waveform estimation, we propose the waveform estimation based on the Green's function integral as follows.

At first, let us consider the electric-field waveform after propagating through a finite aperture. This model is an approximation of the scattering from a rectangular target. We assume that the waveform which passed through the finite rectangular aperture can be regarded as the approximation of the scattered waveform with the opposite sign from a rectangular perfect electric conductor plate whose size is the same as that of the aperture. We assume the coordinates shown in Fig. 6 and set the rectangular aperture on the plane ($y = 0$). We set the transmitted and received antenna at $(0, -r, 0)$ and $(0, r, 0)$, respectively. We assume that r is longer enough than the wavelength. Under this assumption,

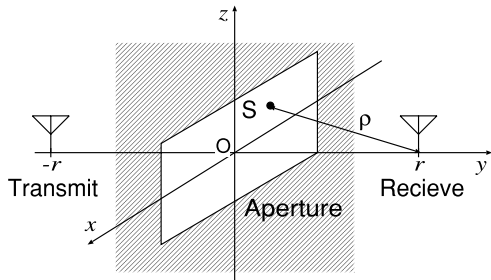


Fig. 6 Arrangement of the antenna and the rectangular aperture in 3-dimensional model.

the electric field of the wave propagating through an aperture in a 3-dimensional problem is approximated by the following equation [7].

$$E(r) \approx \frac{jk}{2\pi} E'_0 \int_S g(2\rho) dS, \quad (7)$$

where k is the wave number, S is the surface of the aperture, g is the Green's function, ρ is the distance from the aperture to the received antenna, $E(r)$ is the electric field at the received antenna, and E'_0 is the electric field on the aperture. This approximation does not include the influences of the scattered waves due to induced current at the edge of the aperture. However, these influences become small except for the region near the edge.

In a 2-dimensional problem and TE mode waves, we assume that the length of the aperture along z axis is infinite. In this model, we approximate the electric field of the received antenna as

$$E(r) \approx \sqrt{\frac{jk}{2\pi}} E'_0 \int_l g(2\rho) ds, \quad (8)$$

where $E(r)$ is the amplitude of z component of the entire electric field at $(0, r, 0)$. E'_0 is that on the aperture. l is the range of the aperture boundary. g is the Green's function of 2-dimensional problem as given by

$$g(\rho) = \frac{j}{4} H_0^{(2)}(k\rho), \quad (9)$$

where $H_0^{(2)}(x)$ is the 0th order Hankel's function of the 2nd kind.

We expand this principle to the scattered waveform estimation. We assume that the scattered waveform from the plate is the same as the passing wave through the aperture. We utilize E_0 which expresses the electric field of the transmitted waveform instead of E'_0 , and approximate the scattered waveform from the finite plate as

$$E(r) \approx K \sqrt{jk} E_0 \int_l g(2\rho) ds, \quad (10)$$

where K is a constant.

By utilizing this principle, we calculate the transfer function by calculating the integral of the Green's function in Eq. (10). By applying this transfer function to the transmitted waveform $E_0(\omega)$, we calculate the scattered waveform $F(\omega, X)$ in the frequency domain as

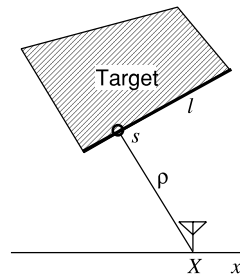


Fig. 7 The integral path of the target boundary at $X \in X_S$.

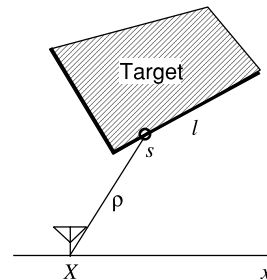


Fig. 8 The integral path of the target boundary at $X \in X_E$.

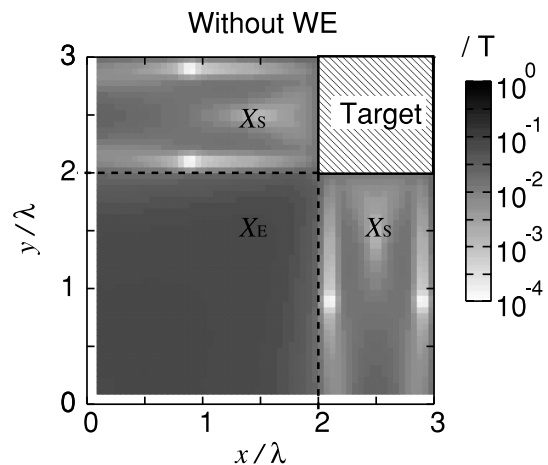


Fig. 9 Estimation errors of the time of arrival without WE.

$$F(\omega, X) = K \sqrt{jk} E_0(\omega) \int_l g(2\rho) ds, \quad (11)$$

where we set l in the case of $X \in X_S$ as shown in Fig. 7, and set l in the case of $X \in X_E$ as shown in Fig. 8. Here, we approximate the edge diffraction waveform as the summation of the two specular reflection waveforms from the planar boundaries making the edge. This method enables us to compensate the frequency change depending on the Fresnel zone size in each frequency.

4.2 Accuracy of the Scattered Waveform Estimation

We examine the accuracy of the scattered waveform estimation. Here, we assume the true shape parameters are known and evaluate the accuracy of the waveform estimation. We call this waveform estimation at WE (Waveform

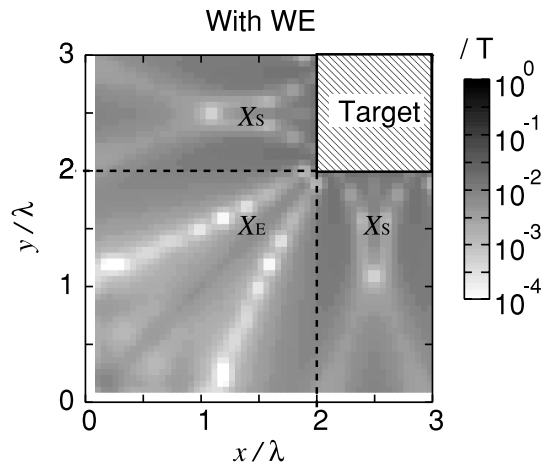


Fig. 10 Estimation errors of the time of arrival with WE.

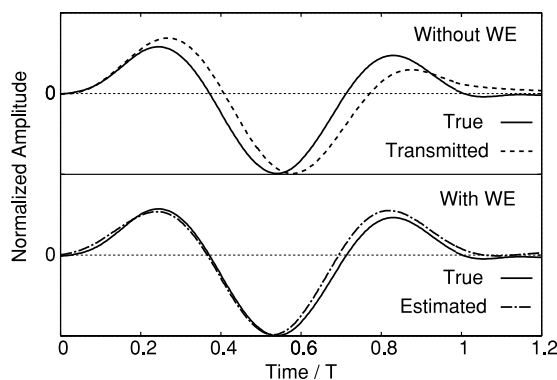


Fig. 11 Waveform estimation in region X_S at $(2.5\lambda, 1.0\lambda)$ without WE (upper panel), and with WE (lower panel).

Estimation), as follows. We assume the target is a square pillar at $2.0 \leq x, y \leq 3.0$ in Fig. 9 and set the antennas at the two regions X_E and X_S except for the region of the target as shown in Fig. 9. Figures 9 and 10 show the errors of the time of arrival modified by T with the matched filter of the transmitted waveform and the estimated one, respectively. Without WE, the errors in the region X_E are very large because the edge diffraction waveform is close to the integral waveform of the transmitted one. On the other hand, the accuracy of the time of arrival in X_E with WE is remarkably improved by 10 times compared to that without WE. In the region X_S , we also see that the accuracy is improved by 5 times except for the region near the edge. In the region near the edge, we confirm that the waveform estimation method is less effective as shown in Fig. 10. This is because the scattered waveform is strongly influenced by the scattered wave due to induced currents at the edge points of the target.

Figures 11 and 12 show the examples of the estimated and the scattered waveform at $(2.5\lambda, 1.0\lambda)$ and $(1.0\lambda, 1.0\lambda)$ in Fig. 9, respectively. These figures show that both the specular reflection and the edge diffraction waveforms are accurately estimated by WE.

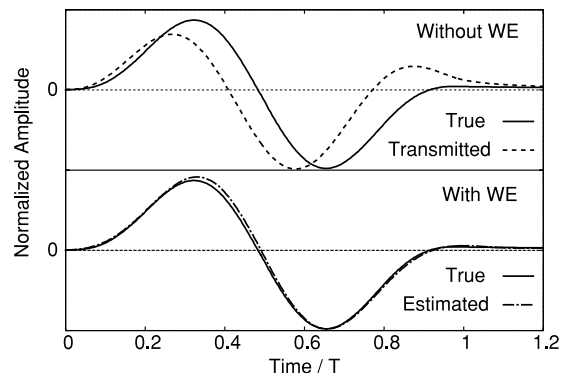


Fig. 12 Same as Fig. 11, but in region X_E at $(1.0\lambda, 1.0\lambda)$.

5. Evaluation of Target Shape Estimation Accuracy

5.1 Evaluation with a Numerical Simulation

In this section, we evaluate the accuracy of the proposed method by numerical simulations. In the simulations, we set 40 antennas along x -axis for $0.125\lambda \leq X \leq 5.0\lambda$ whose interval d is 0.125λ . We assume that the target is a perfect conductor. We set the iteration number as $M=5$, and the true shape parameter as $\mathbf{Z}_t = (2.5\lambda, 1.0\lambda, \pi/4, -\pi/4, 1.1\lambda, 1.1\lambda)$.

First, we assume a noiseless environment. Figure 13 shows the received signals at each antenna location. Figure 14 shows the estimated target boundary. We estimate the target boundary more accurately with WE than without WE. Figures 15 and 16 show the estimation errors of the edge position and the target angle, respectively, for each iteration. These figures show that the shape estimation with WE achieves the edge position accuracy of $2.0 \times 10^{-3}\lambda$ and the target angle accuracy of 2.5×10^{-3} rad. Here, the accuracy of the target angle is worse than the initial shape in the shape estimation without WE. This is because the mean accuracy of the time of arrival at X_{S_i} is worse than that at X_i which decides the initial target angles. These results show that the shape estimation with WE achieves 10 times improvement in the estimation accuracy compared to that without WE. The calculation time of the shape estimation is within 0.2 sec for Xeon 2.8 GHz processors. Also this method can be applied for the polygonal target by increasing the shape parameters \mathbf{Z}_t .

Next, we evaluate the proposed method in a noisy environment. We add white noise to the received signal at each antenna location. Figures 17 and 18 show the estimation errors of the edge position and the target angle versus S/N , respectively. Here we define S/N as

$$S/N = \frac{1}{\sigma_N^2(X_{\max} - X_{\min})} \int_{X_{\min}}^{X_{\max}} \max_Y |s(X, Y)|^2 dX, \quad (12)$$

where X_{\max} and X_{\min} is the maximum and minimum antenna location, respectively, and σ_N is the standard deviation of the noise. In these figures, we conclude that the shape estimation with WE achieves 10 times improvement in the es-

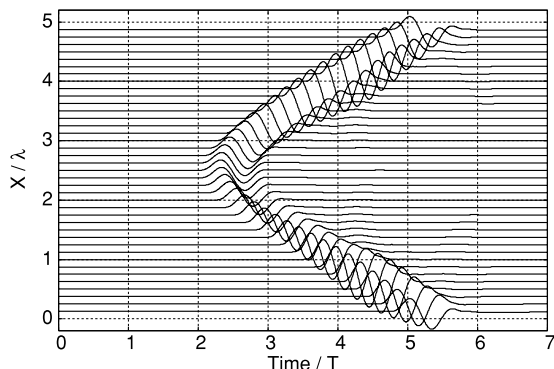


Fig. 13 Received signals at each antenna location.

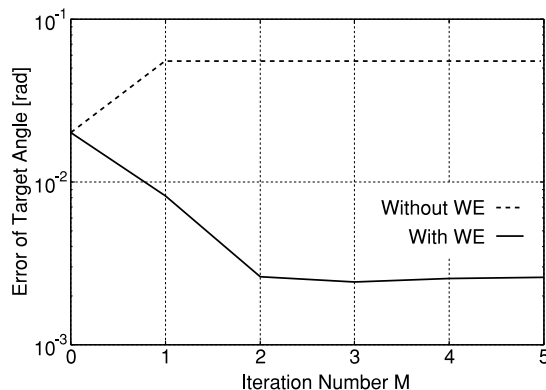


Fig. 16 Estimation errors of the target angle.

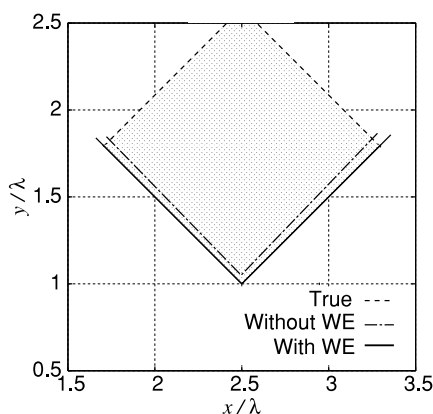


Fig. 14 Estimated boundary of the target.

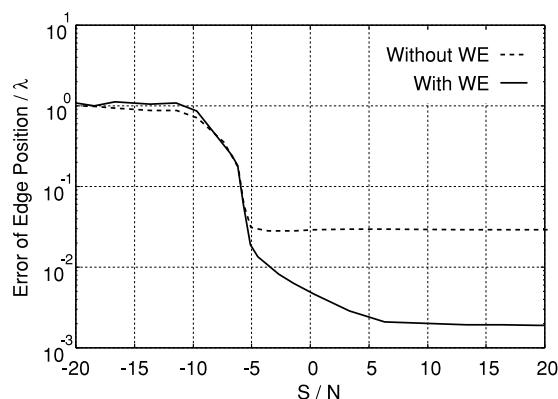


Fig. 17 Estimation errors of the edge position versus S/N.

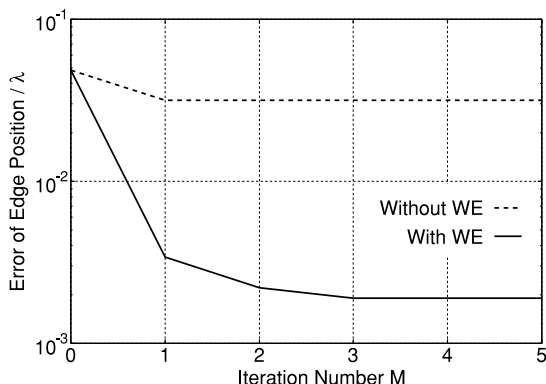


Fig. 15 Estimation errors of the edge position.

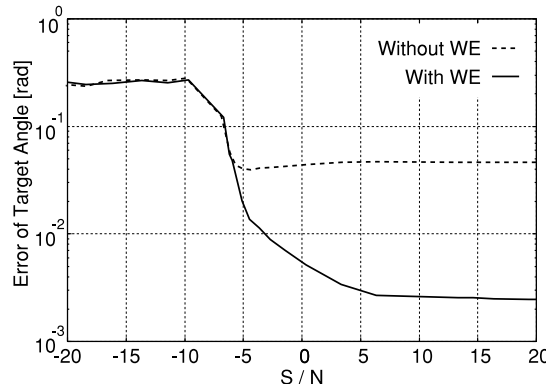


Fig. 18 Estimation errors of the target angle versus S/N.

timization accuracy of both the edge position and the target angle for $S/N > 5$ dB. The estimation accuracy is not good for $S/N < -5$ dB independently of the waveform estimation process. Waveform estimation is not effective if the initial estimation fails due to a noise because it utilizes these parameters as initial values. Therefore, both the two methods give almost the same estimation under this noisy environment. Second, in general, S/N of the UWB signal is limited to a small value. However we utilize the received signal, so we can easily obtain S/N over 5 dB with coherent integrations, as is the case of the experiment presented below.

5.2 Evaluation with an Experiment

In this section, we examine the performance of the proposed method by experiments. We utilize a UWB signal with the center frequency of 3.2 GHz and the 10 dB bandwidth of 2.1 GHz. The antenna has an elliptic polarization whose ratio of the major axis to the minor one is about 17 dB, and the direction of the polarimetric axis of the antenna is along the z axis. The 3 dB beamwidth of the antenna is about 90° . The target is made of stainless steel sheet.

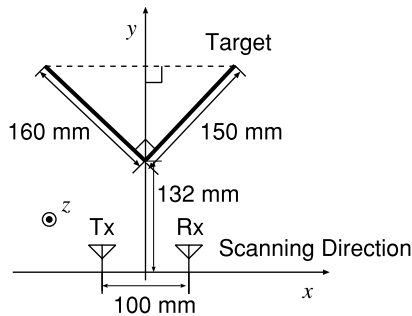


Fig. 19 Arrangement of the antenna and the target in the experiment.

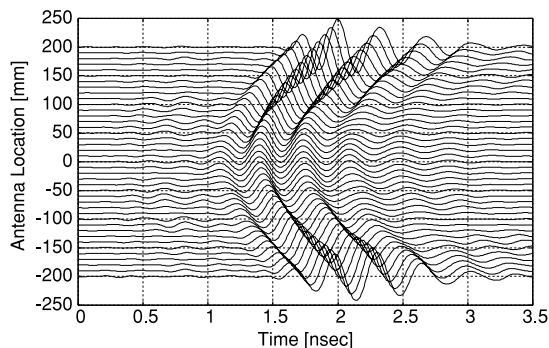


Fig. 20 Scattered waveforms at each antenna location in the experiment.

Figure 19 shows the location of the antenna and the target. We utilize a bistatic antenna whose separation in x direction is 100 mm. We define the antenna location $(X, 0, 0)$ as the center point of the two antennas. Under the assumption of 2-dimensional problem, we set the target whose length in the z direction is sufficiently long. Furthermore, we scan the transmitting antenna in the z direction in order to obtain a 2-dimensional scattered waveforms. In TE mode wave, we assume that the 2-dimensional scattered waveform is approximated as the summation of the 3-dimensional scattered waveforms along the z axis at a fixed $(X, 0, 0)$. Under this assumption, we calculate the 2-dimensional scattered waveform $R(X, t)$ as

$$R(X, t) = \sum_{i=0}^N r(X, z_i, t), \quad (13)$$

where $r(X, z_i, t)$ is the scattered waveform from the transmitting point $(X, 0, z_i)$ to the receiving point $(X, 0, 0)$, N is fixed to 40, and the sampling interval is fixed to 10 mm. The data is coherently averaged for 1024 times to enhance the S/N. We scan the transmitting antenna for the range of $-200 \text{ mm} \leq z \leq 200 \text{ mm}$. We measure the direct wave entering from the transmitting antenna at the absence of the target, and eliminate this component from the received signals to obtain the scattered waveform.

Figure 20 shows the scattered waveforms at each antenna location where S/N is 45 dB. Figure 21 shows the estimated waveform at $X = 0 \text{ mm}$ when we give the true parameter. As shown in this figure, the estimated waveform is much closer to the scattered waveform

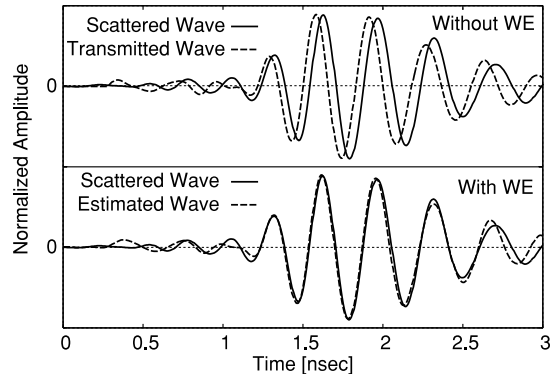


Fig. 21 Waveform estimation for the experimental data without WE (upper panel) and with WE (lower panel).

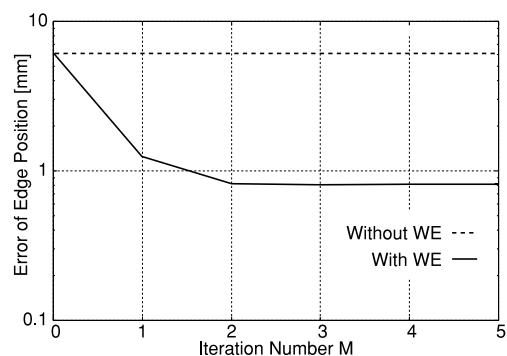


Fig. 22 Estimated errors of the edge position in the experiment.

than the transmitted one. To evaluate the shape estimation, we modify $\tau_a(X, x, y) = \sqrt{(x - X - d_B/2)^2 + y^2} + \sqrt{(x - X + d_B/2)^2 + y^2}$ in Eq. (4), where d_B is the separation of the bistatic antennas. We also give the true value to $(\phi_1, \phi_2, W_1, W_2)$ at the evaluation. Figure 22 shows the estimation accuracy of the edge position. In this figure, the accuracy of the edge position improves from 6.0 mm to 0.8 mm. These experimental results show that the shape estimation with WE is effective in the real environment. In our numerical simulation, the proposed method achieves the accuracy of the edge location of $2.0 \times 10^{-3} \lambda$. In the experiments, it achieves the accuracy of the edge location $8.5 \times 10^{-4} \lambda$ ($\lambda = 93.75 \text{ mm}$). In these results, the accuracy of the experiments is slightly better than that of the numerical simulation. This is because we assumed that the edge angle is known for evaluations with the experiments.

6. Conclusion

We proposed an accurate target shape estimation method in this paper. At first, we proposed an iterative algorithm for the target shape estimation with a scattered waveform estimation. We utilized the waveform estimation with the Green's function integral. We applied this principle to both of the specular reflection and the edge diffraction waveform estimation. With numerical simulations, we confirmed that the shape estimation with WE achieves a high accuracy in

the estimation of the time of arrival. This simple diffraction model cannot express the scattered waveform perfectly. However this model can estimate the time of arrival accurately enough by roughly estimating the frequency characteristic of the waveform deformation. Therefore it is effective for shape estimation.

We evaluated the proposed method in a noiseless environment by numerical simulations, and achieved the accuracy of the edge position $2.0 \times 10^{-3} \lambda$ and the target angle 2.5×10^{-3} rad. In a noisy environment, we achieved 10 times improvement in the estimation accuracy than that without WE for $S/N > 5$ dB. These evaluations showed 10 times improvement of the estimation accuracy in both of the edge position and the target angle. We also evaluated the proposed method in experiments with a UWB signal generator. The experimental results showed that the proposed method estimates the edge position with the accuracy of 0.8 mm for $S/N = 45$ dB. We showed that the calculation time of the proposed method is within 0.2 sec, where iteration number is 5, and achieved a fast and an accurate shape estimation. The calculation time of the proposed method is shorter than that of the conventional method [3] which needs 6.7 sec for a ThunderBird 1.0 GHz Athlon to obtain 2-dimensional image. Although our proposed method is limited to the target shape with edges, the accuracy of the edge position is better than the conventional methods [1]–[4] whose accuracy is over 0.1λ . The proposed method cannot be applied to a curved target but it can be readily extended to a polygonal target. The proposed method can be applied to measurement techniques in an indoor environment where we see many polygonal targets, such as doors, corner of walls, staircases, furniture, etc.

Acknowledgment

We thank Dr. Tomohiko Mitani at the Research Institute for Sustainable Humanosphere, Kyoto University, Japan, for his valuable advices. This work is supported in part by the 21st Century COE Program (Grant No. 14213201).

References

- [1] T. Sato, K. Takeda, T. Nagamatsu, T. Wakayama, I. Kimura, and T. Shinbo, "Automatic signal processing of front monitor radar for tunneling machines," *IEEE Trans. Geosci. Remote Sens.*, vol.35, no.2, pp.354–359, 1997.
- [2] T. Sato, T. Wakayama, and K. Takemura, "An imaging algorithm of objects embedded in a lossy dispersive medium for subsurface radar data processing," *IEEE Trans. Geosci. Remote Sens.*, vol.38, no.1, pp.296–303, 2000.
- [3] T. Takenaka, H. Jia, and T. Tanaka, "Microwave imaging of an anisotropic cylindrical object by a forward-backward time-stepping method," *IEICE Trans. Electron.*, vol.E84-C, no.12, pp.1910–1916, Dec. 2001.
- [4] C. Chiu, C. Li, and W. Chan, "Image reconstruction of a buried conductor by the genetic algorithm," *IEICE Trans. Electron.*, vol.E84-C, no.12, pp.1946–1951, Dec. 2001.
- [5] T. Sakamoto and T. Sato, "A target shape estimation algorithm for pulse radar systems based on boundary scattering transform," *IEICE Trans. Commun.*, vol.E87-B, no.5, pp.1357–1365, May 2004.
- [6] T. Sakamoto and T. Sato, "A phase compensation algorithm for high-resolution pulse radar systems," *IEICE Trans. Commun.*, vol.E87-B, no.6, pp.1631–1638, June 2004.
- [7] K. Maeda and I. Kimura, *Gendai denji hadou ron*, Ohmsha, pp.70–72, 1984.



Shouhei Kidera received the B.E. degree from Kyoto University in 2003 and the M.E. degree at Graduate School of Informatics, Kyoto University in 2005. He is currently studying for the Ph.D. degree at Graduate School of Informatics, Kyoto University. His current research interest is in digital signal processing. He is a member of the IEEE.



Takuya Sakamoto was born in Nara, Japan in 1977. Dr. Sakamoto received his B.E. degree from Kyoto University in 2000, and his M.I. and Ph.D. degrees from Graduate School of Informatics, Kyoto University in 2002 and 2005, respectively. He is a research associate in the Department of Communications and Computer Engineering, Graduate School of Informatics, Kyoto University. His current research interest is in signal processing for UWB pulse radars. He is a member of the IEEE and the IEEJ.



Satoshi Sugino received B.S. and M.S. Degrees from Kyoto University in 1982 and 1984, respectively. He joined Matsushita Electric Works, Ltd., Osaka, Japan in 1984, where he has been engaged in the development of ICs. From 1989 to 1991, he was with Applied Electronics Lab. of Stanford University, where he worked on the CMOS device simulator development. He is currently working on the development of short-range wireless devices and their RF IC technologies.



Toru Sato received his B.E., M.E., and Ph.D. degrees in electrical engineering from Kyoto University, Kyoto, Japan in 1976, 1978, and 1982, respectively. He has been with Kyoto University since 1983 and is currently a Professor in the Department of Communications and Computer Engineering, Graduate School of Informatics. His major research interests have been system design and signal processing aspects of atmospheric radars, radar remote sensing of the atmosphere, observations of precipitation using radar and satellite signals, radar observation of space debris, and signal processing for subsurface radar signals. Dr. Sato was awarded Tanakadate Prize in 1986. He is a member of the Society of Geomagnetism and Earth, Planetary and Space Sciences, the Japan Society for Aeronautical and Space Sciences, the Institute of Electrical and Electronics Engineers, and the American Meteorological Society.